

Lithospheric deformation in the Canadian Appalachians: evidence from shear wave splitting

Amy Gilligan,¹ Ian D. Bastow,¹ Emma Watson,¹ Fiona A. Darbyshire,² Vadim Levin,³ William Menke,⁴ Victoria Lane,⁵ David Hawthorn,^{5,6} Alistair Boyce,¹ Mitchell V. Liddell¹ and Laura Petrescu¹

¹*Department of Earth Science and Engineering, Imperial College London, London SW7 2AZ, United Kingdom. E-mail: a.gilligan@imperial.ac.uk*

²*GEOTOP, Université du Québec à Montréal, Montréal, Québec, Canada*

³*Department of Earth and Planetary Sciences, Rutgers University, Piscataway, NJ, USA*

⁴*Lamont-Doherty Earth Observatory, Columbia University, Palisades, NY, USA*

⁵*SEIS-UK, University of Leicester, Leicester LE1 7RH, United Kingdom*

⁶*BGS Murchison House, W Mains Rd, Edinburgh EH9 3LA, United Kingdom*

Accepted 2016 May 31. Received 2016 May 27; in original form 2016 January 11

SUMMARY

Plate-scale deformation is expected to impart seismic anisotropic fabrics on the lithosphere. Determination of the fast shear wave orientation (ϕ) and the delay time between the fast and slow split shear waves (δt) via SKS splitting can help place spatial and temporal constraints on lithospheric deformation. The Canadian Appalachians experienced multiple episodes of deformation during the Phanerozoic: accretionary collisions during the Palaeozoic prior to the collision between Laurentia and Gondwana, and rifting related to the Mesozoic opening of the North Atlantic. However, the extent to which extensional events have overprinted older orogenic trends is uncertain. We address this issue through measurements of seismic anisotropy beneath the Canadian Appalachians, computing shear wave splitting parameters (ϕ , δt) for new and existing seismic stations in Nova Scotia and New Brunswick. Average δt values of 1.2 s, relatively short length scale (≥ 100 km) splitting parameter variations, and a lack of correlation with absolute plate motion direction and mantle flow models, demonstrate that fossil lithospheric anisotropic fabrics dominate our results. Most fast directions parallel Appalachian orogenic trends observed at the surface, while δt values point towards coherent deformation of the crust and mantle lithosphere. Mesozoic rifting had minimal impact on our study area, except locally within the Bay of Fundy and in southern Nova Scotia, where fast directions are subparallel to the opening direction of Mesozoic rifting; associated δt values of > 1 s require an anisotropic layer that spans both the crust and mantle, meaning the formation of the Bay of Fundy was not merely a thin-skinned tectonic event.

Key words: Body waves; Seismic anisotropy; Continental tectonics: compressional; Continental tectonics: extensional; North America.

INTRODUCTION

Plate-scale deformation can lead to the development of an anisotropic fabric within the lithosphere (e.g. Helffrich 1995) through the alignment of olivine crystals in the upper mantle (e.g. Zhang & Karato 1995; Bystricky *et al.* 2000; Tommasi *et al.* 2000). When a shear wave travels through an anisotropic medium it is split into two orthogonal shear waves, one travelling faster than the other (e.g. Silver 1996). Measurements of the polarisation direction of the fast wave (ϕ) and the delay time between the fast and slow waves (δt) can then be used to characterise the anisotropic medium.

Core shear waves such as SKS and SKKS (hereafter referred to as SKS) are well suited for studying shear wave splitting and the anisotropic properties of the upper mantle directly beneath a seismic station. They are radially polarised, *P*-to-*S* conversions formed at the core–mantle boundary that preserve no source-side anisotropy (Savage 1999; Long & Silver 2009).

The Canadian Appalachians have experienced multiple episodes of deformation during the Phanerozoic (e.g. van Staal & Barr 2012). A series of Palaeozoic accretionary collisions took place on the margin of Laurentia, prior to the Laurentia–Gondwana collision that formed the supercontinent Pangea. In the Mesozoic, rifting related to the opening of the North Atlantic affected the eastern

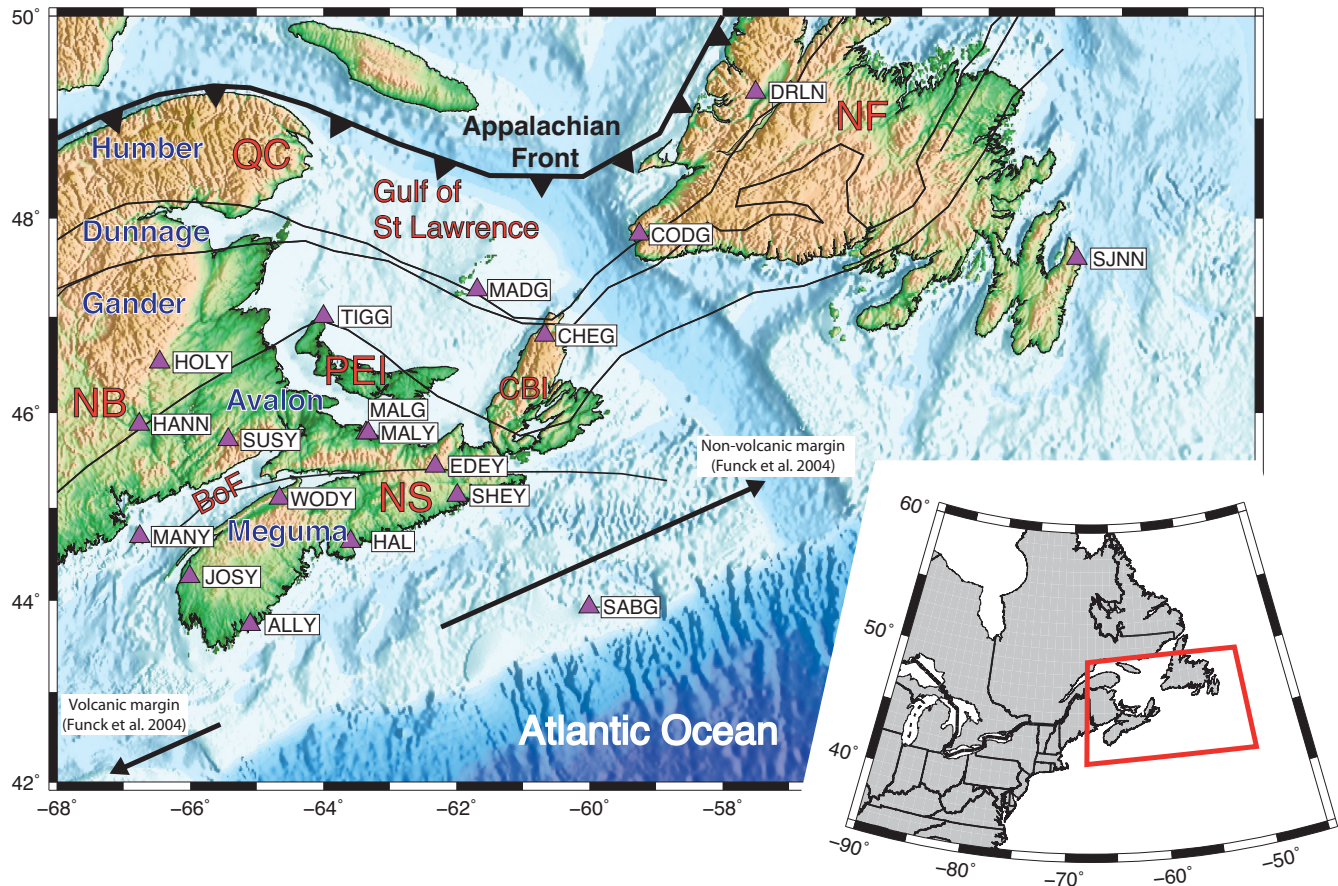


Figure 1. Locations of broad-band seismic stations (magenta triangles), boundaries separating the Humber, Dunnage, Gander, Avalon and Meguma regions (thin black lines) and the Appalachian Front (thick black line). Inset map shows the location of the study region, marked as a red box, within eastern North America. QC—Quebec, NB—New Brunswick, NS—Nova Scotia, PEI—Prince Edward Island, CBI—Cape Breton Island, NF—Newfoundland and BoF—Bay of Fundy.

edge of this region, one consequence of which was the formation of the Bay of Fundy (e.g. Withjack *et al.* 1995; Fig. 1).

Previous studies of shear wave splitting parameters in south-east Canada revealed little correspondence between orientations of anisotropic fabrics and asthenospheric flow beneath the Canadian Appalachians (Darbyshire *et al.* 2015). Fossil lithospheric anisotropic fabrics are thus likely to exert first-order control on the observations. However, data from only a small number of seismic stations in the Canadian Appalachians have been used to establish this hypothesis, rendering the plate-scale tectonic evolution of the region poorly constrained in space and time. For example, whether or not the Mesozoic formation of the Fundy Basin was a thin-skinned, ‘crustal’ event, or one that also affected the mantle lithospheric mantle, remains poorly understood.

To address these issues, we analyse broad-band seismic data from a combined network of new and existing seismic stations centred on the Bay of Fundy, to compute shear wave splitting parameters (ϕ , δt) for the region. After consideration of proposed mantle flow directions from absolute plate motion (APM) and geodynamic modelling results (Darbyshire *et al.* 2015), we compare the orientation of the fast direction to geological trends from the Appalachian orogenies, rifting in the Bay of Fundy, and extension related to the opening of the North Atlantic. In doing so, we assess the orientation and depth extent of deformation and whether rifting-related anisotropic fabrics have overprinted older orogenic anisotropic fabrics.

TECTONIC SETTING

The Canadian Appalachians formed from the accretion of a series of oceanic arcs and continental fragments to the southeast margin of Laurentia during the Palaeozoic. The region can be divided into five principal tectonostratigraphic zones (Williams 1979; Fig. 1), although it should be noted that some comprise distinct tectonic elements themselves (e.g. van Staal & Barr 2012). To the northwest, the Humber Margin, was the edge of Laurentia when Dunnage zone material was accreted during the Ordovician, closing the Taconic Seaway. Both zones comprise material that was on the Laurentian side of the Iapetus Ocean.

The three southeastern zones, Ganderia, Avalonia and Meguma, were continental fragments that separated from Gondwana during the Early Palaeozoic. Ganderia collided with the composite edge of Laurentia during the Silurian, closing the Iapetus Ocean and Avalonia accreted during the Early Devonian Arcadian Orogeny. Finally, Meguma, a terrane only found in present-day southern Nova Scotia, collided with the Avalonian edge of Laurentia in the Carboniferous.

Terminal collision between Laurentia and Gondwana occurred in the Mid-Carboniferous and Early Permian during the Alleghanian Orogeny, and led to the formation of the supercontinent Pangea. The Canadian Appalachians were relatively unaffected by Alleghanian Orogeny deformation (van Staal & Barr 2012) and are thus a good location to study structures related to the earlier accretionary tectonic phases.

Table 1. Stacked split results.

| Station | Net | Lat (°) | Lon (°) | ϕ (°) | σ_ϕ (°) | δt (s) | $\sigma_{\delta t}$ | # | Data period |
|---|---------|---------|---------|------------|-------------------|----------------|---------------------|---|--|
| ALLY | IC | 43.74 | -65.10 | -84 | 1.25 | 1.43 | 0.05 | 2 | 2013 September–2014 July; 2015 May–2015 August |
| CHEG | CNSN | 46.81 | -60.67 | -56 | 12.75 | 1.00 | 0.23 | 1 | 2005 October–2015 October |
| CODG | POLARIS | 47.84 | -59.25 | 58 | 4.75 | 1.02 | 0.24 | 1 | 2005 October–2008 October |
| EDEY | IC | 45.44 | -62.32 | 83 | 1.75 | 1.23 | 0.03 | 5 | 2013 September–2015 August |
| HAL | CNSN | 44.64 | -63.59 | 67 | 2.5 | 0.90 | 0.02 | 4 | 2008 August–2015 October |
| HANN | POLARIS | 45.88 | -66.77 | 71 | 2.5 | 0.93 | 0.03 | 2 | 2013 January–2015 October |
| HOLY | IC | 46.53 | -66.46 | 33 | 2.5 | 1.40 | 0.08 | 3 | 2013 September–2015 August |
| MALG | POLARIS | 45.79 | -63.33 | 71 | 1 | 1.85 | 0.13 | 2 | 2005 October–2008 October |
| MALY | IC | 45.79 | -63.36 | 83 | 5.25 | 1.05 | 0.06 | 3 | 2013 September–2015 August |
| MANY | IC | 44.69 | -66.76 | -75 | 1.5 | 1.48 | 0.03 | 3 | 2013 September–2013 November; 2014 May–2015 August |
| SHEY | IC | 45.13 | -61.99 | -89 | 1.75 | 1.00 | 0.03 | 3 | 2013 September–2015 August |
| SUSY | IC | 45.72 | -65.43 | 58 | 5.00 | 1.23 | 0.06 | 2 | 2013 September–2015 August |
| TIGG | POLARIS | 47.00 | -64.00 | -55 | 6.75 | 0.68 | 0.09 | 4 | 2005 September–2007 November |
| WODY | IC | 45.10 | -64.66 | 85 | 0.75 | 1.33 | 0.02 | 6 | 2013 September–2015 August |
| Splitting parameters from Darbyshire <i>et al.</i> (2015) | | | | | | | | | |
| BATG | POLARIS | 47.23 | -66.06 | -86 | 5.00 | 0.53 | 0.03 | 6 | |
| GBN | CNSN | 45.41 | -61.51 | -84 | 1.50 | 0.68 | 0.03 | 7 | |
| GGN | CNSN | 45.12 | -66.84 | 67 | 1.00 | 1.03 | 0.03 | 9 | |
| LMN | CNSN | 45.85 | -64.81 | 76 | 1.75 | 1.15 | 0.06 | 5 | |

Notes: IC: Imperial College Maritimes network; POLARIS: Portable Observatories for Lithospheric Analysis and Research Investigating Seismicity; CNSN: Canadian National Seismograph Network; #: Number of splitting measurements used in a stack and σ : one standard deviation. The splitting parameters obtained for individual events can be found in Table S1 in the Supporting Information and null events are recorded in Table S2 in the Supporting Information.

During the Mid-Triassic to Early Jurassic, NW-SE oriented rifting formed the Bay of Fundy (Withjack *et al.* 1995; Withjack *et al.* 2010). Rifting reactivated Palaeozoic thrusts as normal faults, and resulted in the deposition of syn-rift non-marine sedimentary rocks and the eruption of tholeiitic basalts (Withjack *et al.* 1995). Fundy Basin extension ceased with the opening of the North Atlantic in the Early-to-Mid Jurassic. The rifted margin shows variation offshore of Nova Scotia: the margin is volcanic to the southwest, but non-volcanic to the northeast of Nova Scotia and Newfoundland (Keen and Potter 1995; Funck *et al.* 2004). Since the Cretaceous, the Canadian Appalachians have been tectonically quiet.

DATA AND METHODS

We use data from 19 broad-band seismic stations deployed in the Canadian Appalachians (Table 1 and Fig. 1) in Nova Scotia, New Brunswick, Newfoundland and Quebec. Of these, nine stations are from the Imperial College Maritimes network in Nova Scotia and New Brunswick, deployed between 2013 September and 2015 August. These stations consisted of Guralp CMG-3TP seismometers with associated Guralp digitisers and GPS timing. The remaining stations consist of six temporary POLARIS stations (Portable Observatories for Lithospheric Analysis and Research Investigating Seismicity: Eaton *et al.* 2005) that operated for periods of 2–3.5 yr, and four permanent stations from the Canadian National Seismograph Network (CNSN).

Earthquakes that occurred between 2005 October and 2015 October, with magnitudes ≥ 6.0 and epicentral distances $\geq 88^\circ$ were selected from the global catalogue. This distance range was chosen to isolate SKS core phases from other direct S phases to focus our analysis on receiver-side mantle anisotropy. Seismograms were filtered using a zero-phase, two-pole, Butterworth bandpass filter with corner frequencies 0.04 and 0.3 Hz. Seismograms were visually inspected and waveforms with high signal-to-noise ratio, where an SKS or SKKS phase was clearly visible, were selected for further analysis.

When an SKS phase exhibits shear wave splitting, particle motion is elliptical because a proportion of the energy exists on the tangential component (e.g. Fig. 2). If shear wave splitting does not occur, the particle motion will be linear and no energy appears on the tangential component, resulting in a ‘null’ measurement (e.g. Fig. 3). A null may result from the material that the wave passes through being azimuthally isotropic, multiple layers of anisotropy cancelling out (Barruol & Hoffmann 1999), or if the backazimuth of the incoming earthquake is parallel or perpendicular to the fast polarisation direction.

We measure the fast polarisation direction (ϕ) and the delay time between the fast and slow shear waves (δt) using the approach of Teanby *et al.* (2004), which is based on the methodology of Silver & Chan (1991). Horizontal-component seismograms are rotated and time-shifted to minimise the second eigenvalue of the covariance matrix for particle motion within a window around the SKS phase. This is equivalent to linearising particle motion, and minimising the energy on the tangential component seismogram. We make measurements for 100 different windows around the SKS phase, and use cluster analysis to determine the most stable splitting parameters. Only measurements where the difference between the backazimuth and source polarisation direction of the SKS phase is $\leq 20^\circ$ are accepted, thus avoiding spurious results that could be associated with anomalies in the deep lower mantle (e.g. Restivo & Helffrich 2006). We obtain 40 high-quality split measurements and 30 null measurements from 25 earthquakes (Tables S1 and S2, Supporting Information and Fig. 4). It should be noted that many of the seismic stations were located close to the coast, in a relatively high noise environment, and some stations (e.g. ALLY, JOSY and MANY) only operated for the short timespan of ~ 1 yr.

RESULTS

Fig. 2 shows an example of a split measurement from station EDEY; Fig. 3 is an example null measurement from station SJNN. Splitting parameters for individual station-event pairs are shown in

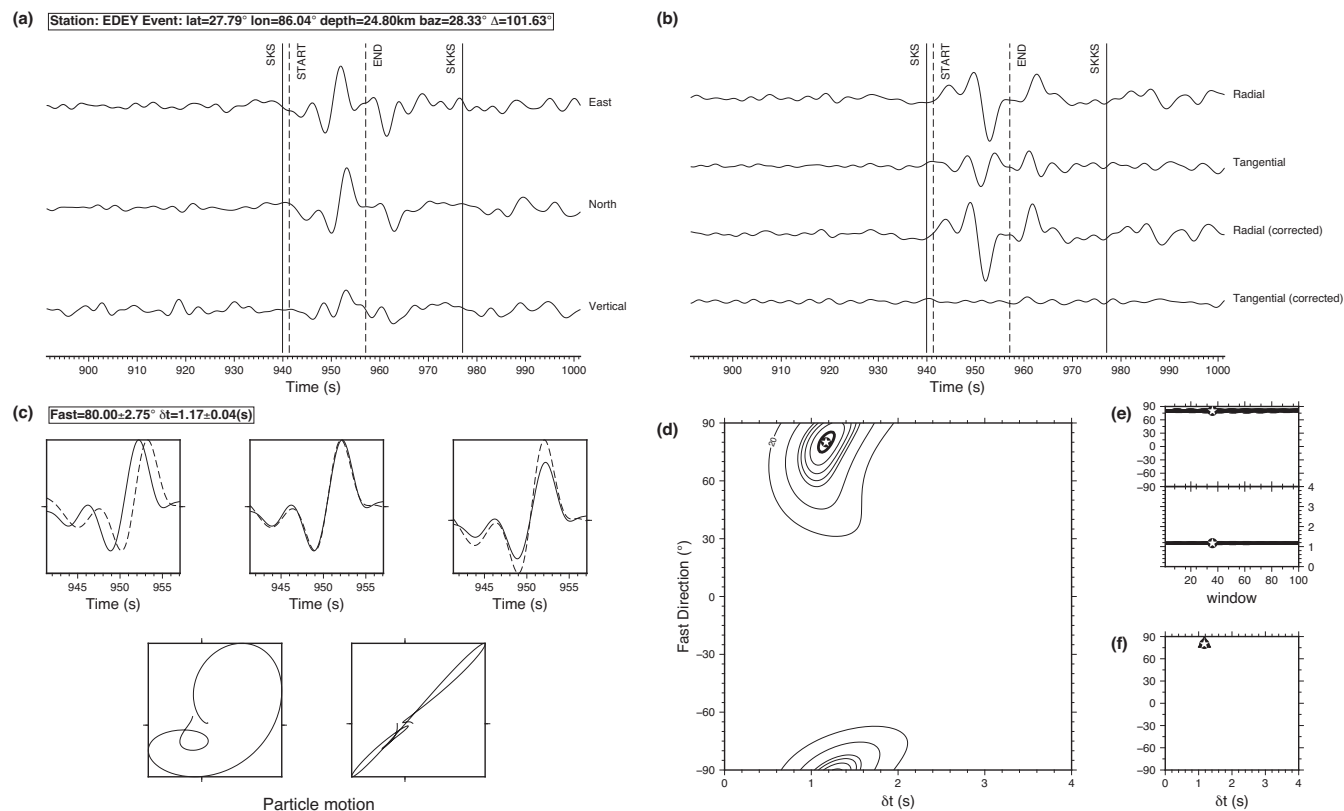


Figure 2. An example of a good splitting measurement at station EDEY. (a) The original three component seismogram showing the SKS phase and the window used. (b) The radial and tangential components before (top two) and after correction (bottom two). There is no energy on the corrected tangential component. (c) Top three images show the match between the fast (dashed line) and slow (solid line) waveforms: left is prior to correction (amplitudes normalised) and centre and right are after correction, normalised and true amplitudes, respectively. Left: the bottom two images show the elliptical particle motion prior to correction and right: the linearised particle motion after correction. (d) Error and uncertainty calculation (contour labels indicate multiples of one sigma). Here, a stable result and a well-constrained 95 per cent confidence contour (thick line) indicate a robust measurement. (e) Measurements of ϕ and δt obtained from 100 different analysis windows plotted against window number. (f) Cluster analysis of splitting parameters obtained from the 100 windows. Good results are stable over a large number of windows. In (d), (e) and (f) the star marks the values of ϕ and δt taken for this station/event pair.

Figs S1–S4 in the Supporting Information and summarised in Fig. S5 and Table S2 in the Supporting Information.

At stations where splitting parameters show no significant back-azimuthal variation, mantle anisotropy is characterised as a single, homogenous, horizontal layer; we thus adopt the stacking approach of Restivo & Helffrich (2006) to obtain a single pair of splitting parameters. Data coverage is insufficient to resolve the complex patterns of shear wave splitting variation associated with multiple or dipping anisotropic layers.

Results are summarised in Fig. 4 and Table 1. Delay times range from 0.7 s (TIGG) to 1.85 s (MALG), but most fall within $\delta t = 0.9$ –1.4 s. Consistent fast directions can be observed within some groups of stations on a 200–300 km length scale, but changes over short distances (<100 km) are also evident. One of the most striking is the change from a SE–NW fast direction for stations ALLY (southern Nova Scotia) and MANY (Bay of Fundy) to a SW–NE fast direction for stations in southern New Brunswick (Fig. 4). Fast directions across northern Nova Scotia are generally \sim WSW–ENE, but those observed for stations CHEG (Cape Breton Island) and TIGG (Prince Edward Island) are NW–SE. The fast direction changes once again to SW–NE on the southern tip of Newfoundland (Fig. 4).

At stations SABG, JOSY, MADG, SJNN and DRLN only null measurements were found. For JOSY, MADG and DRLN, the earthquake backazimuths yielding these results were either parallel or perpendicular to the fast directions observed at neighbouring

stations (ALLY and MANY, TIGG and CHEG and CODG, respectively). Given the 90° ambiguity inherent in null measurements, it is reasonable to assume that the null directions are either perpendicular or parallel to the fast direction of anisotropy at these stations. However, the limited backazimuthal coverage means we cannot preclude the presence of multiple, cancelling layers of anisotropy (e.g. Barruol & Hoffmann 1999) beneath these stations.

DISCUSSION

Causes of seismic anisotropy and comparisons with previous studies

Seismic anisotropy in the Earth results from the alignment of minerals in the crust and/or mantle, the preferential alignment of fluid or melt (e.g. Blackman & Kendall 1997), alternating sequences of subparallel layers of rocks of different seismic velocities (periodic transverse layering; Backus 1962), or some combination thereof. We exclude melt alignment as a source of anisotropy in the Canadian Appalachians, since the region last experienced magmatism during the Mesozoic (van Staal & Barr 2012). Mantle anisotropy therefore most likely results from the alignment of olivine crystals, olivine being the most abundant mineral in the upper mantle and highly anisotropic. Shear stresses can lead to the development of crystallographic preferred orientation (CPO) of olivine, where the

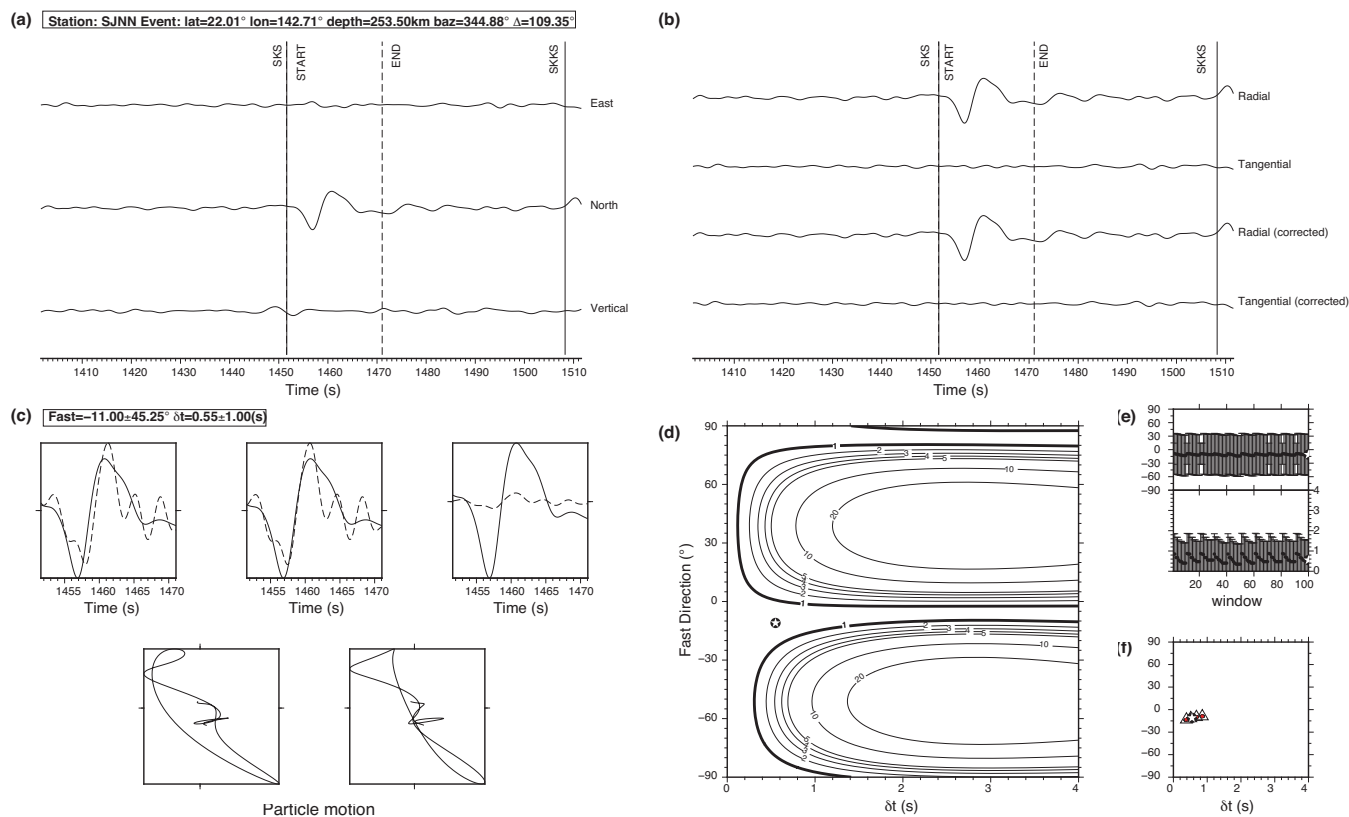


Figure 3. An example of a null result at the station SJNN. (a)–(f) as in Fig. 2. Note in (b) the lack of energy on the tangential component before and after correction and in (c) the linear particle motion before and after analysis.

a -axis is aligned to an orientation related to deformation (e.g. Zhang & Karato 1995; Bystricky *et al.* 2000; Tommasi *et al.* 2000).

Processes that could lead to the development of anisotropic fabric include: asthenospheric flow in the direction of APM (e.g. Bokelmann & Silver 2002), asthenospheric flow around a cratonic root (e.g. Bormann *et al.* 1993; Assumpção *et al.* 2006) and frozen-in fossil anisotropy within the lithosphere from the last deformation event (e.g. Silver & Chan 1988; Vauchez & Nicolas 1991; Bastow *et al.* 2007).

Periodic transverse layering is likely a source of anisotropy at crustal depths, however the continental crust typically only accounts for only 0.1–0.3 s (Silver 1996) or 0.1–0.5 s (Barruol & Mainprice 1993) of SKS splitting observations, so our δt values (mean $\delta t = 1.2$ s) require a mantle contribution. Estimates of anisotropic layer thickness can be made from the relationship $L \approx (\delta t \times Vs) / dVs$ (e.g. Helffrich 1995), where L is layer thickness, Vs is shear velocity and dVs is average percentage anisotropy. Taking a dVs of 4 per cent, an upper limit of the degree of anisotropy prevalent in the upper 200 km of the Earth (Savage 1999) and a Vs in the range 4.48 km s^{-1} (mantle velocities from ak135; Kennett *et al.* 1995) to 4.65 km s^{-1} (average cratonic lithospheric mantle velocities in SE Canada; Schaeffer & Lebedev 2014, Yuan *et al.* 2014), our mean $\delta t = 1.2$ s corresponds to a layer thickness of 134–140 km, not dissimilar to the ~ 150 –175 km estimates for lithospheric thickness in the Canadian Appalachians (Schaeffer & Lebedev 2014). Similarly, if we assume that the average 1.2 s of splitting we observe is accrued in the region's 150–175 km thick lithosphere (e.g. Schaeffer & Lebedev 2014), the uppermost mantle beneath our network would be, on average, 3.1–3.7 per cent anisotropic, a reasonable estimate for lithospheric anisotropy when compared to other stud-

ies worldwide (e.g. Savage 1999). Further, the distances over which splitting parameters change (in several cases < 100 km) is smaller than the width of the first Fresnel zone at the base of the lithosphere (~ 150 km).

There are four published SKS splitting measurements in our study area from Darbyshire *et al.* (2015; Fig. 4 and Table 1). These show good agreement with the results we obtain from nearby stations. The nearest station to our region analysed by Barruol *et al.* (1997) (station CBM in Maine) has a similar fast direction to that of station HOLY, and is subparallel to the strike of Palaeozoic Appalachian orogenic structures.

Many of the ϕ measurements obtained from the northern US Appalachians to the southwest of our study region by Barruol *et al.* (1997) are E-W oriented. Subsequent modelling of anisotropy in the New England region (Levin *et al.* 1999; Levin *et al.* 2000; Yuan & Levin 2014) finds that it is best explained by two distinct layers: a lower layer in the asthenosphere paralleling APM and an upper layer in the lithosphere that is perpendicular to the main geological trends in the region. It is argued that this upper layer may be a result of a fabric developed due to the loss of the lower part of the lithosphere at some point after the assemblage of the Appalachians. Multiple layers of anisotropy, including the presence of anisotropy in the lithosphere, are further supported by estimates of anisotropic parameters made using splitting measurements and full waveform analysis (e.g. Yuan & Romanowicz 2010; Yuan *et al.* 2011).

Long *et al.* (2015) recently conducted an SKS splitting study of the eastern US using data from the Transportable Array seismic stations. In the southern Appalachians, from Alabama to Pennsylvania, they see a strong correlation between ϕ and the strike of the mountain chain, including a rotation in ϕ coincident with a bend in

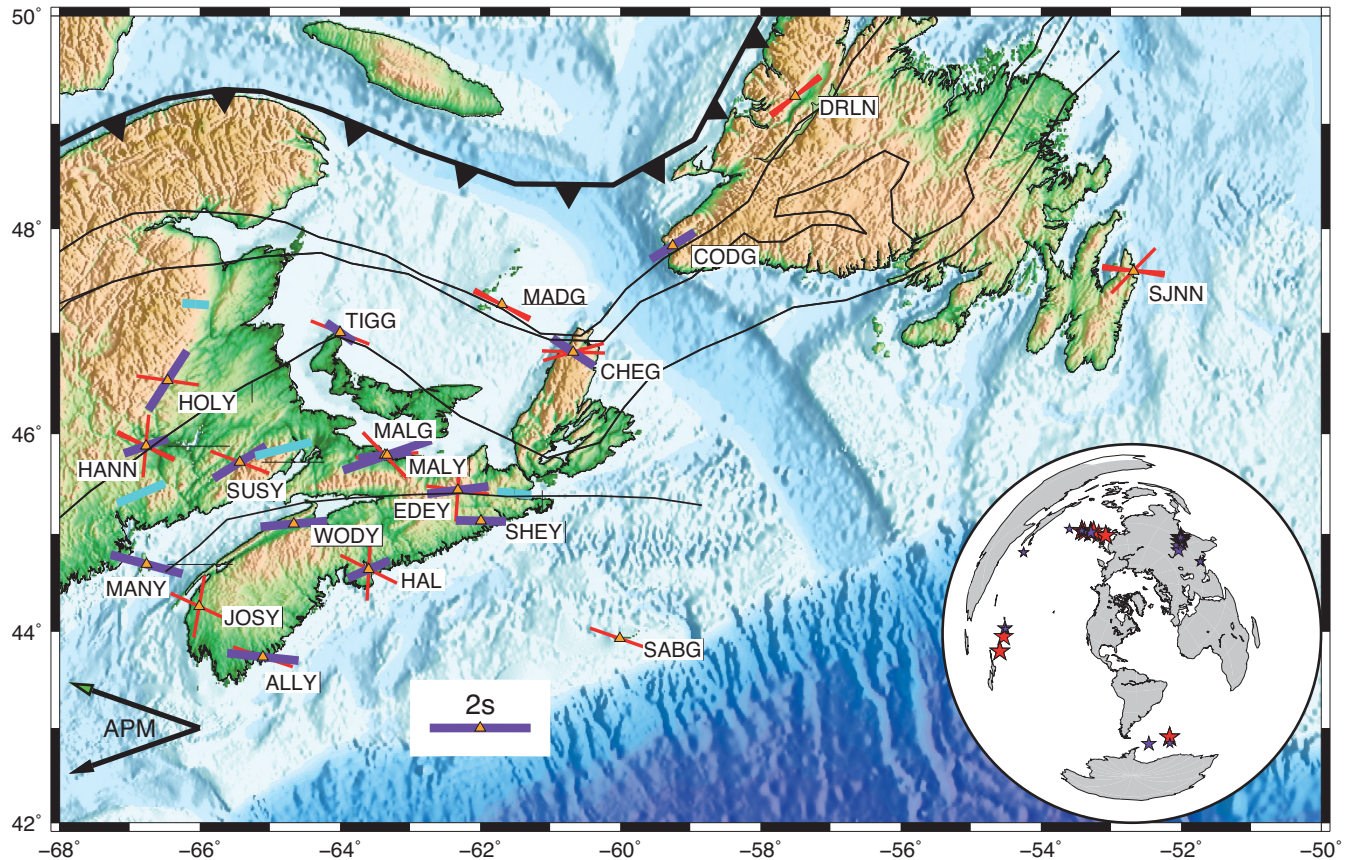


Figure 4. Stacked shear wave splitting parameters from the stations in this study (purple bars) and from Darbyshire *et al.* (2015) (cyan bars). Red bars are null measurements. APM: absolute plate motion from the HS3-Nuvel-1A model of Gripp & Gordon (2002) in the hotspot reference frame (black arrow) and the NNR-MORVEL (no-net-rotation) model of DeMets *et al.* (2010) (green arrow). Inset map shows the location of earthquakes used, red stars are events where null measurements were obtained and purple stars are events where split measurements were obtained.

topography. They argue in this region that the primary contribution to anisotropy is from the lithosphere. In the region closest to our study region, directly to the west and south, their results are more complex. Averaged over a relatively large area, the average ϕ direction is 77° , however there is significant variation over relatively short distances, which they also argue suggests a lithospheric component to the observed anisotropy. In neither of these two regions do they observe a consistent alignment to APM.

Role of plate motion and mantle flow

Splitting measurements from southern New Brunswick and southern Newfoundland show some agreement with the APM direction from the HS3-NUVEL 1A (hotspot) model (Gripp & Gordon 2002), however there is no consistent correlation with APM direction across the whole region. Similarly, while the fast direction observed in southern Nova Scotia and in the Bay of Fundy parallels the NNR-MORVEL (no-net-rotation) model (DeMets *et al.* 2010) there is again no consistent correlation throughout the Maritimes. Furthermore, the North American Plate is moving relatively slowly ($17\text{--}22\text{ mm yr}^{-1}$), slower than the $\sim 40\text{ mm yr}^{-1}$ that Debayle & Ricard (2013) suggest is the necessary plate velocity for basal drag fabrics to develop based on their global comparison of APM and anisotropic fast directions. Anisotropy resulting from APM is, therefore, unlikely to be the dominant cause of the observed anisotropy.

Darbyshire *et al.* (2015) compare splitting parameters to mantle flow predictions of Forte *et al.* (2015). In the model that best simu-

lates the lithospheric thickness in Appalachian Canada, radial flow dominates over horizontal flow. This would result in null measurements for the majority of seismic stations in this region: this clearly is not the case for most stations. Taking into account our estimates of anisotropic layer thickness and the lack of correlation of APM directions and mantle flow models, a fossil lithospheric hypothesis for Canadian Appalachian mantle anisotropy seems most appropriate.

Backazimuthal coverage of our splitting measurements is limited to a relatively narrow range (Figs S1–S4). Studies with better backazimuthal representation are usually associated with stations that operated for much longer than the 1–3 yr to which we have access (e.g. Levin *et al.* 2000). Although our interpretations are necessarily limited to a single homogenous, horizontal layer of anisotropy, we cannot preclude the possibility of dipping or multiple layers of anisotropy, including an asthenospheric component (e.g. Silver & Savage 1994; Levin *et al.* 2000).

Relationship with tectonic structures

Fast polarisation directions in the Canadian Appalachians are mostly parallel or subparallel to geological trends from the Palaeozoic Appalachian orogenies (Fig. 1). Variations, such as between those in southern New Brunswick and those in Nova Scotia, and between Prince Edward Island, New Brunswick and Newfoundland follow variations in the strike of the boundaries between the different tectonic zones. Agreement between Appalachian trends and fast directions has also been documented elsewhere in the orogen by

Long *et al.* (2015) and in earlier work by Barruol *et al.* (1997). Further, previous SKS splitting studies from other old orogenic belts, such as the Caledonian trends in the UK and Ireland (e.g. Helffrich 1995; Bastow *et al.* 2007) have also noted that olivine CPO tends to parallel the strike of these belts. Much of the anisotropy we observe is thus related to Appalachian tectonic deformation. Splitting delay times of $\delta t > 1$ s point towards plate-scale deformation, coherent in the crust and lithospheric mantle.

The NW-SE fast direction at station MANY in the Bay of Fundy is at a high angle to the trend of Appalachian structures. The Bay of Fundy underwent rifting in a NW-SE direction during the Mid-Triassic to Early Jurassic (e.g. Withjack *et al.* 1995); extensional deformation may thus have overprinted older Appalachian trends. In magma-rich rifts, fast directions are typically rift-parallel (e.g. Kendall *et al.* 2006), but in magma-poor rifts such as the Rhine Graben (Vinnik *et al.* 1992) and the Baikal rift (Gao *et al.* 1997), they tend to be rift-perpendicular. This is due to the lattice-preferred orientation of lithospheric mantle olivine crystals induced by plate stretching (Nicolas & Christensen 1987). Withjack *et al.* (1995) suggest the Fundy Basin experienced compression in a NW-SE direction from the Early Jurassic to Early Cretaceous. Unlike the earlier rifting, this does not seem to have influenced the lithospheric mantle.

The fast direction for MANY is slightly oblique ($\sim 25^\circ$) to the Bay of Fundy palaeo opening direction. Obliquity between the strike of normal fault networks and opening directions is not uncommon during the development of continental breakup, however. For example, Corti (2008) observes a $\sim 20^\circ$ obliquity in the tectonically active Ethiopian rift. Our observations are thus consistent with the hypothesis that, in the Bay of Fundy, Mesozoic plate-scale extensional tectonics overprinted older Appalachian fossil lithospheric anisotropic fabrics.

The fast direction at ALLY on the Atlantic coast of southern Nova Scotia is similar to MANY, but $\sim 30^\circ$ different to HAL, also located on Nova Scotia's Atlantic coast. The observations at ALLY may, like MANY, be the result of Mesozoic rifting. Although we cannot constrain them, along-axis variations in the strength of the continental lithosphere may explain our observations: weaker lithosphere to the south where the Bay of Fundy formed; stronger lithosphere to the north. Offshore-rifted margin structure lends some support to this hypothesis: seaward dipping reflector sequences are prevalent along the margin in the south, but missing further northeast (Keen & Potter 1995). Funck *et al.* (2004) argue that the Nova Scotian margin becomes increasingly non-volcanic to the northeast, also implying a change in extensional processes along strike. Regardless of the governing factor, we conclude that Mesozoic extensional deformation of the lithosphere in the Canadian Maritimes was plate scale but localised in nature.

CONCLUSIONS

SKS splitting measurements are made at 19 broad-band seismic stations in the Canadian Appalachians. Improved station numbers and density compared to previous studies in this region means we are better able to constrain spatial and temporal variations in lithospheric deformation. The length scale of variations (~ 100 km), average δt of 1.2 s and the lack of correlation with APM directions and asthenospheric flow models suggests that frozen-in lithospheric fabrics dominate the anisotropy in the region. There is good agreement between the fast polarisation directions at most stations and surface geological trends related to the Appalachian orogenies. Palaeozoic accretionary collisions thus likely deformed the crust

and the mantle lithosphere coherently. Later Mesozoic rifting had minimal impact on the Canadian Appalachians outside of the Bay of Fundy and southern Nova Scotia. In these areas, fast directions do not follow Appalachian trends, but are subparallel to the direction of rifting in the Mesozoic. This suggests that Mesozoic rifting affected the entire lithosphere beneath the Bay of Fundy, not just the crust, but its influence was confined to this relatively small area.

ACKNOWLEDGEMENTS

This work was funded by Leverhulme Trust research project grant RPG-2013-332. Imperial College Maritimes network stations were provided through Natural Environment Research Council (NERC) Geophysical Equipment Facility loan 986. Logistical field support was provided by D. Heffler, D. Simpson, and residents of Nova Scotia and New Brunswick. Data for Portable Observatories for Lithospheric Analysis and Research Investigating Seismicity (POLARIS) and Canadian National Seismograph Network stations were downloaded from the Canadian National Data Centre. POLARIS stations were funded by the Canadian Foundation for Innovation, Natural Resources Canada and Industry Canada. FD is supported by Natural Sciences and Engineering Research Council of Canada through the Discovery Grants and Canada Research Chair programmes. AB is funded by the NERC Doctoral Training Partnership: Science and Solutions for a Changing Planet. We thank Thomas Plenefisch and an anonymous reviewer for their comments on this manuscript.

REFERENCES

- Assumpção, M., Heintz, M., Vauchez, A. & Silva, M.E., 2006. Upper mantle anisotropy in SE and Central Brazil from SKS splitting: evidence of asthenospheric flow around a cratonic keel, *Earth planet. Sci. Lett.*, **250**(1), 224–240.
- Backus, G.E., 1962. Long-wave elastic anisotropy produced by horizontal layering, *J. geophys. Res.*, **67**, 4427–4440.
- Barruol, G. & Hoffmann, R., 1999. Upper mantle anisotropy beneath the Geoscope stations, *J. geophys. Res.*, **104**(B5), 10 757–10 773.
- Barruol, G. & Mainprice, D., 1993. A quantitative evaluation of the contribution of crustal rocks to the shear-wave splitting of teleseismic SKS waves, *Phys. Earth planet. Inter.*, **78**(3), 281–300.
- Barruol, G., Silver, P.G. & Vauchez, A., 1997. Seismic anisotropy in the eastern United States: deep structure of a complex continental plate, *J. geophys. Res.*, **102**, 8329–8348.
- Bastow, I.D., Owens, T.J., Helffrich, G. & Knapp, J.H., 2007. Spatial and temporal constraints on sources of seismic anisotropy: Evidence from the Scottish highlands, *Geophys. Res. Lett.*, **34**, L05305, doi:10.1029/2006GL028911.
- Blackman, D.K. & Kendall, J.M., 1997. Sensitivity of teleseismic body waves to mineral texture and melt in the mantle beneath a mid-ocean ridge, *Phil. Trans. R. Soc. Lond., A: Math. Phys. Eng. Sci.*, **355**(1723), 217–231.
- Bokelmann, G. & Silver, P., 2002. Shear stress at the base of shield lithosphere, *Geophys. Res. Lett.*, **29**(23), 2091, doi: 10.1029/2002GL015925.
- Bormann, P., Burghardt, P.T., Makeyeva, L.I. & Vinnik, L.P., 1993. Teleseismic shear-wave splitting and deformations in Central Europe, *Phys. Earth planet. Inter.*, **78**(3), 157–166.
- Bystricky, M., Kunze, K., Burlini, L. & Burg, J.P., 2000. High shear strain of olivine aggregates: rheological and seismic consequences, *Science*, **290**(5496), 1564–1567.
- Corti, G., 2008. Control of rift obliquity on the evolution and segmentation of the main Ethiopian rift, *Nat. Geosci.*, **1**(4), 258–262.
- Darbyshire, F.A., Bastow, I.D., Forte, A.M., Hobbs, T.E., Calvel, A., Gonzalez-Monteza, A. & Schow, B., 2015. Variability and origin of seismic anisotropy across eastern Canada: evidence from shear-wave splitting measurements, *J. geophys. Res.*, **120**, doi:10.1002/2015JB012228.

- Debayle, E. & Ricard, Y., 2013. Seismic observations of large-scale deformation at the bottom of fast-moving plates, *Earth planet. Sci. Lett.*, **376**, 165–177.
- DeMets, C., Gordon, R.G. & Argus, D.F., 2010. Geologically current plate motions, *Geophys. J. Int.*, **181**(1), 1–80.
- Eaton, D.W. *et al.*, 2005. Investigating Canada's lithosphere and earthquake hazards with portable arrays, *EOS, Trans. Am. geophys. Un.*, **86**(17), 169–173.
- Forste, A.M., Simmons, N.A. & Grand, S.P., 2015. Constraints on seismic models from other disciplines—Constraints on 3-D seismic models from global geodynamic observables: implications for the global mantle convective flow, in *Treatise of Geophysics*, Vol. 1, pp. 853–907, eds Romanowicz, B. & Dziewonski, A., Elsevier.
- Funck, T., Jackson, H.R., Loudon, K.E., Dehler, S.A. & Wu, Y., 2004. Crustal structure of the northern Nova Scotia rifted continental margin (eastern Canada), *J. geophys. Res.*, **109**, B09102, doi:10.1029/2004JB003008.
- Gao, S. *et al.*, 1997. SKS splitting beneath continental rift zones, *J. geophys. Res.*, **102**(B10), 22781–22797.
- Gripp, A.E. & Gordon, R.G., 2002. Young tracks of hotspots and current plate velocities, *Geophys. J. Int.*, **150**(2), 321–361.
- Helffrich, G., 1995. Lithospheric deformation inferred from teleseismic shear wave splitting observations in the United Kingdom, *J. geophys. Res.*, **100**(B9), 18195–18204.
- Keen, C.E. & Potter, D.P., 1995. The transition from a volcanic to a nonvolcanic rifted margin off eastern Canada, *Tectonics*, **14**(2), 359–371.
- Kendall, J.M., Piliidou, S., Keir, D., Bastow, I.D., Stuart, G.W. & Ayele, A., 2006. Mantle upwellings, melt migration and the rifting of Africa: insights from seismic anisotropy, *Geol. Soc. Lond. Spec. Publ.*, **259**(1), 55–72.
- Kennett, B.L.N., Engdahl, E.R. & Buland, R., 1995. Constraints on seismic velocities in the Earth from traveltimes, *Geophys. J. Int.*, **122**(1), 108–124.
- Levin, V., Menke, W. & Park, J., 1999. Shear wave splitting in the Appalachians and the Urals: a case for multilayered anisotropy, *J. geophys. Res.*, **104**(B8), 17 975–17 993.
- Levin, V., Park, J., Brandon, M.T. & Menke, W., 2000. Thinning of the upper mantle during late Paleozoic Appalachian orogenesis, *Geology*, **28**(3), 239–242.
- Long, M.D. & Silver, P.G., 2009. Shear wave splitting and mantle anisotropy: measurements, interpretations, and new directions, *Surv. Geophys.*, **30**(4–5), 407–461.
- Long, M.D., Jackson, K.G. & McNamara, J.F., 2015. SKS splitting beneath Transportable Array stations in eastern North America and the signature of past lithospheric deformation, *Geochem. Geophys. Geosyst.*, **16**, doi:10.1002/2015GC006088.
- Nicolas, A. & Christensen, N.I., 1987. Formation of anisotropy in upper mantle peridotites—a review, in *Composition, Structure and Dynamics of the Lithosphere–Asthenosphere System*, pp. 111–123, eds Fuchs, K. & Froidevaux, C., American Geophysical Union.
- Restivo, A. & Helffrich, G., 2006. Core–mantle boundary structure investigated using SKS and SKKS polarization anomalies, *Geophys. J. Int.*, **165**(1), 288–302.
- Savage, M.K., 1999. Seismic anisotropy and mantle deformation: what have we learned from shear waves, *Rev. Geophys.*, **37**(1), 65–106.
- Schaeffer, A.J. & Lebedev, S., 2014. Imaging the North American continent using waveform inversion of global and USArray data, *Earth planet. Sci. Lett.*, **402**, 26–41.
- Silver, P.G., 1996. Seismic anisotropy beneath the continents: probing the depths of geology, *Annu. Rev. Earth planet. Sci.*, **24**, 385–432.
- Silver, P.G. & Chan, W.W., 1988. Implications for continental structure and evolution from seismic anisotropy, *Nature*, **335**, 34–39.
- Silver, P.G. & Chan, W.W., 1991. Shear wave splitting and subcontinental mantle deformation, *J. geophys. Res.*, **96**(16), 16 429–16 454.
- Silver, P.G. & Savage, M.K., 1994. The interpretation of shear-wave splitting parameters in the presence of two anisotropic layers, *Geophys. J. Int.*, **119**(3), 949–963.
- Teanby, N.A., Kendall, J.M. & Van der Baan, M., 2004. Automation of shear-wave splitting measurements using cluster analysis, *Bull. seism. Soc. Am.*, **94**(2), 453–463.
- Tommasi, A., Mainprice, D., Canova, G. & Chastel, Y., 2000. Viscoplastic self-consistent and equilibrium-based modeling of olivine lattice preferred orientations: implications for the upper mantle seismic anisotropy, *J. geophys. Res.*, **105**(B4), 7893–7908.
- van Staal, C.R. & Barr, S.M., 2012. Lithospheric architecture and tectonic evolution of the Canadian Appalachians and associated Atlantic margin, in *Tectonic Styles in Canada: The LITHOPROBE Perspective*, Vol. 49, pp. 41–95, eds Percival, J.A., Cook, F.A. & Clowes, R.M., Geological Association of Canada, Special Paper.
- Vaucher, A. & Nicolas, A., 1991. Mountain building: strike-parallel motion and mantle anisotropy, *Tectonophysics*, **185**(3), 183–201.
- Vinnik, L.P., Makeyeva, L.I., Milev, A. & Usenko, A.Y., 1992. Global patterns of azimuthal anisotropy and deformations in the continental mantle, *Geophys. J. Int.*, **111**(3), 433–447.
- Williams, H., 1979. Appalachian orogen in Canada, *Can. J. Earth Sci.*, **16**(3), 792–807.
- Withjack, M.O., Olsen, P.E. & Schlische, R.W., 1995. Tectonic evolution of the Fundy rift basin, Canada: evidence of extension and shortening during passive margin development, *Tectonics*, **14**(2), 390–405.
- Withjack, M.O., Baum, M.S. & Schlische, R.W., 2010. Influence of preexisting fault fabric on inversion-related deformation: a case study of the inverted Fundy rift basin, southeastern Canada, *Tectonics*, **29**, TC6004, doi:10.1029/2010TC002744.
- Yuan, H. & Levin, V., 2014. Stratified seismic anisotropy and the lithosphere–asthenosphere boundary beneath eastern North America, *J. geophys. Res.*, **119**(4), 3096–3114.
- Yuan, H. & Romanowicz, B., 2010. Lithospheric layering in the North American craton, *Nature*, **466**(7310), 1063–1068.
- Yuan, H., French, S., Cupillard, P. & Romanowicz, B., 2014. Lithospheric expression of geological units in central and eastern North America from full waveform tomography, *Earth planet. Sci. Lett.*, **402**, 176–186.
- Yuan, H., Romanowicz, B., Fischer, K.M. & Abt, D., 2011. 3-D shear wave radially and azimuthally anisotropic velocity model of the North American upper mantle, *Geophys. J. Int.*, **184**(3), 1237–1260.
- Zhang, S. & Karato, S.I., 1995. Lattice preferred orientation of olivine aggregates deformed in simple shear, *Nature*, **375**(6534), 774–777.

SUPPORTING INFORMATION

Additional Supporting Information may be found in the online version of this paper:

Figures S1–S4. The backazimuthal dependence of ϕ and δt across the network as recorded in Table S1 (split measurements, purple squares) for stations with more than one pair of splitting parameters. Solid vertical lines show the backazimuths of earthquakes that yielded null measurements (Table S2).

Figure S5. Individual shear wave splitting parameters for stations in the Canadian Appalachians. Purple headed arrows are high-quality split measurements (Table S1), red crosses are null measurements (Table S2). APM: absolute plate motion from the HS3-Nuvel-1A model of Gripp & Gordon (2002) in the hotspot reference frame (black arrow) and the NNR-MORVEL (no-net-rotation) model of DeMets *et al.* (2010) (green arrow). Inset map: earthquake locations; red stars: earthquakes for which null measurements were obtained and purple stars: earthquakes for which splitting parameters were obtained successfully.

Table S1. Split measurements.

Table S2. Null measurements.

(<http://gji.oxfordjournals.org/lookup/suppl/doi:10.1093/gji/ggw207/-/DC1>).

Please note: Oxford University Press is not responsible for the content or functionality of any supporting materials supplied by the authors. Any queries (other than missing material) should be directed to the corresponding author for the paper.